EGU23-15366

Optimizing simulated oxygen variability, circulation, and export in the subpolar North Atlantic Ocean using BGC-Argo & ship-based observations

Lauren Moseley[1] (laurenm@ldeo.columbia.edu), Galen A. McKinley[1], Dustin Carroll[2,3], Raphael Dussin[4], Dimitris Menemenlis[5], An T. Nguyen[6]

[1]Lamont-Doherty Earth Observatory of Columbia University, [2]Moss Landing Marine Laboratories, [3]San José State University, [4]NOAA Geophysical Fluid Dynamics Laboratory, [5]Jet Propulsion Laboratory, California Institute of Technology, [6]University of Texas at Austin

A

Introduction

- Many ocean models predict oxygen loss as oceans continue to warm, but the magnitude of this loss varies widely across models[1]
- Intense air-sea gas exchange and wintertime deep convection in the subpolar North Atlantic (SPNA) are critical to the ocean oxygen inventory[2,3]
- BGC-Argo floats and GLODAP hydrography offer expanding biogeochemical insight for ocean models

Methods

- We use a data-constrained physical state estimate[4] coupled to the BLING biogeochemical model[5] (ASTE-BGC) to reconstruct the time-evolving 3-D ocean state
- We apply a Green's functions approach[6] (**Table 1**) to constrain ASTE-BGC to in-situ biogeochemical data over 2002–2017 (**Fig. 1**) and reduce model-data misfit (**Fig. 3**)
- We evaluate the optimized model simulation against independent data constraints (**Fig. 4**)

C

Conclusions and Next Steps

- The Green's functions-based optimization is underway and will next target BGC initial conditions to further minimize model-data misfit
- Model-data misfit was most effectively minimized for the BGC-Argo O_2 dataset ($RMSE_{v1-v0}$ = +17%) (**Fig. 2**)
- The optimized ASTE-BGC model will next be used to construct SPNA O_2 budgets to examine the recent interannual variability of air-sea gas exchange, transport, mixing, and biological production

References

1. Keeling et al. 2010, Annu. Rev. Mar. Sci.
2. McKinley et al. 2004, Global Biogeochem. Cy.
3. Rhein et al. 2017, Philos. T. R. Soc.
4. Nguyen et al. 2021, JAMES.
5. Verdy & Mazloff 2017, J. Geophys. Res. Oceans.
6. Carroll et al. 2020, JAMES.

Over 275,000 GLODAPv2 and BGC-Argo observations were used to **improve simulated biogeochemistry in the Labrador Sea**

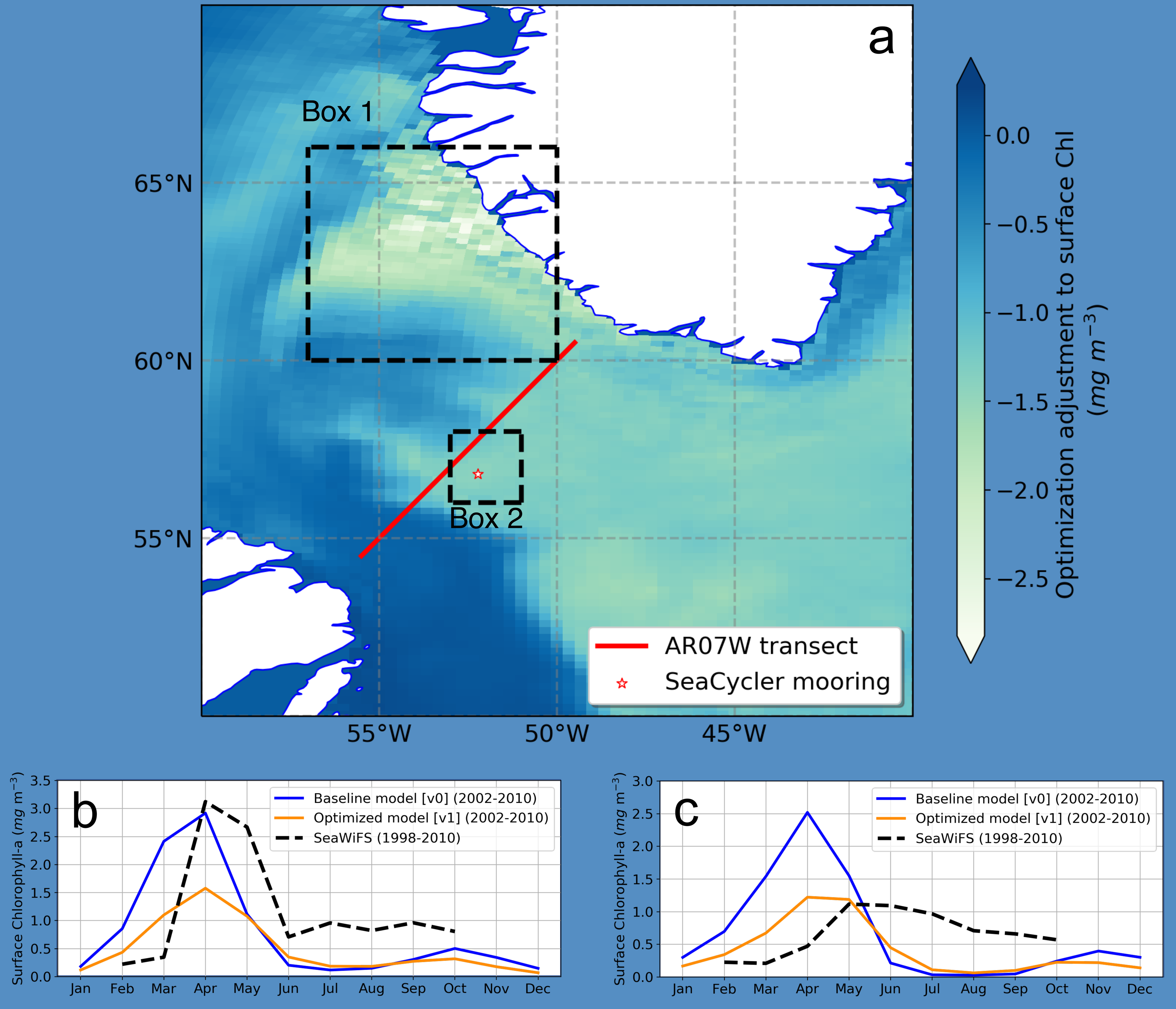

Figure 4. (a) Difference in mean climatological April surface chlorophyll (Chl-a) between the optimized ASTE-BGC model and the baseline ASTE-BGC model (2002–2017), where light green indicates the optimization's largest minimization of surface Chl-a; (b) 2-D averaged monthly climatological surface Chl-a of the baseline model (blue), optimized model (orange), and SeaWiFS observations within Box 1, the region of highest productivity in the Labrador Sea (60–66ºN, 50–57ºW); (c) the same 2-D-averaged monthly climatological surface Chl-a within Box 2 (56–58ºN, 51–53ºW).

B

Results

1. Green's functions optimization description

Table 1. Baseline ASTE-BGC model configuration, five perturbation (±10%) experiments to BLING biogeochemical parameters, and the Green's functions-derived solution of optimal parameter values

		Baseline model (**v0**)	Green's functions perturbation experiments					Optimized model (**v1**)
			exp1	exp2	exp3	exp4	exp5	
BLING parameters	Phytoplankton growth rate (P_0^C)	1.70 x 10^{-5}	1.53 x 10^{-5} **(-10%)**					2.69 x 10^{-5}
	Phytoplankton mortality rate (λ_0)	2.20 x 10^{-6}		2.42 x 10^{-6} **(+10%)**				4.66 x 10^{-6}
	Fraction of small phytoplankton biomass converted to detritus (ϕ_S)	0.18			0.198 **(+10%)**			0.316
	Fraction of large phytoplankton biomass converted to detritus (ϕ_L)	1				0.9 **(-10%)**		0.683
	Nitrate uptake half-saturation constant (k_{NO3})	2.05 x 10^{-3}					1.84 x 10^{-3} **(-10%)**	0.403

2. BGC-Argo (O_2 & NO_3) and GLODAP (O_2, NO_3, PO_4, DIC & Alk)

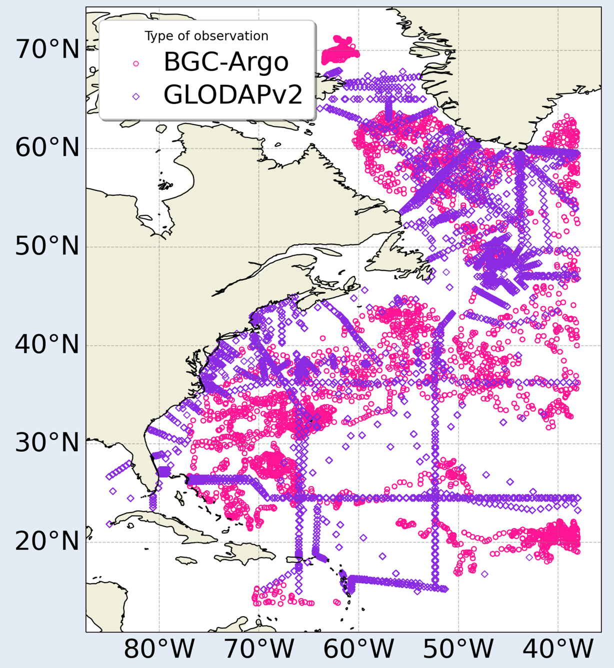

Figure 1. Spatial extent of the BGC-Argo float (N~107,000) & GLODAP cruise (N~168,000) data constraints.

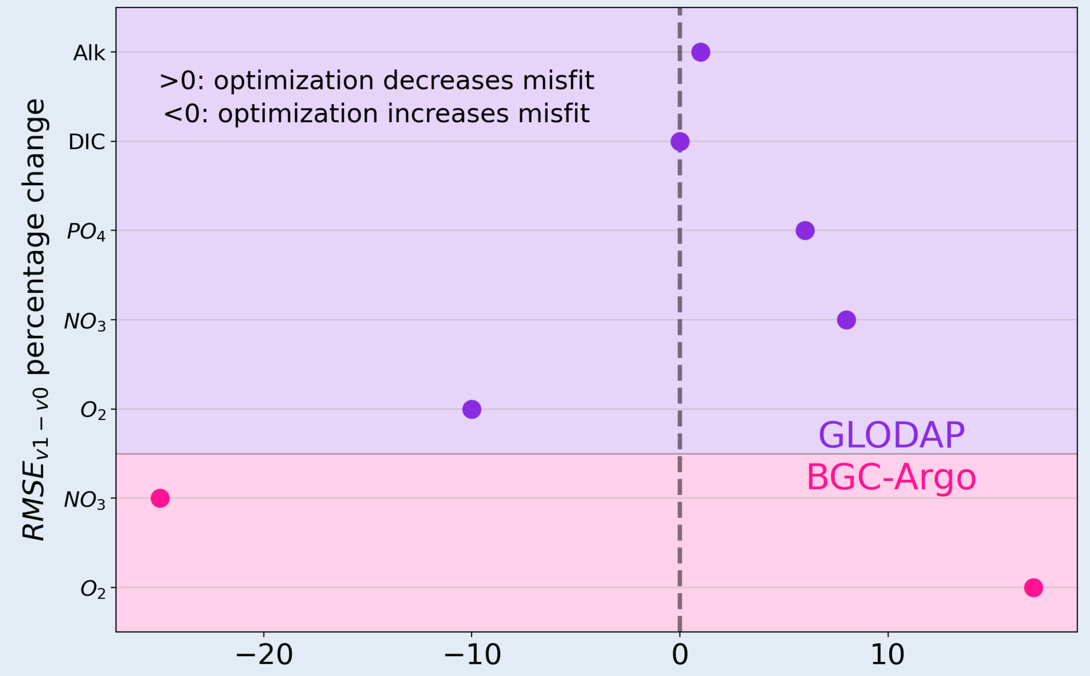

Figure 2. Difference in root mean square error (RMSE), for the 3-D-averaged vertical profile, between observational datasets and the baseline model (v0) & optimized model (v1).

3. Evaluating the optimized model (v1) and the baseline model (v0) in horizontal (latitude/longitude) and vertical (depth) space

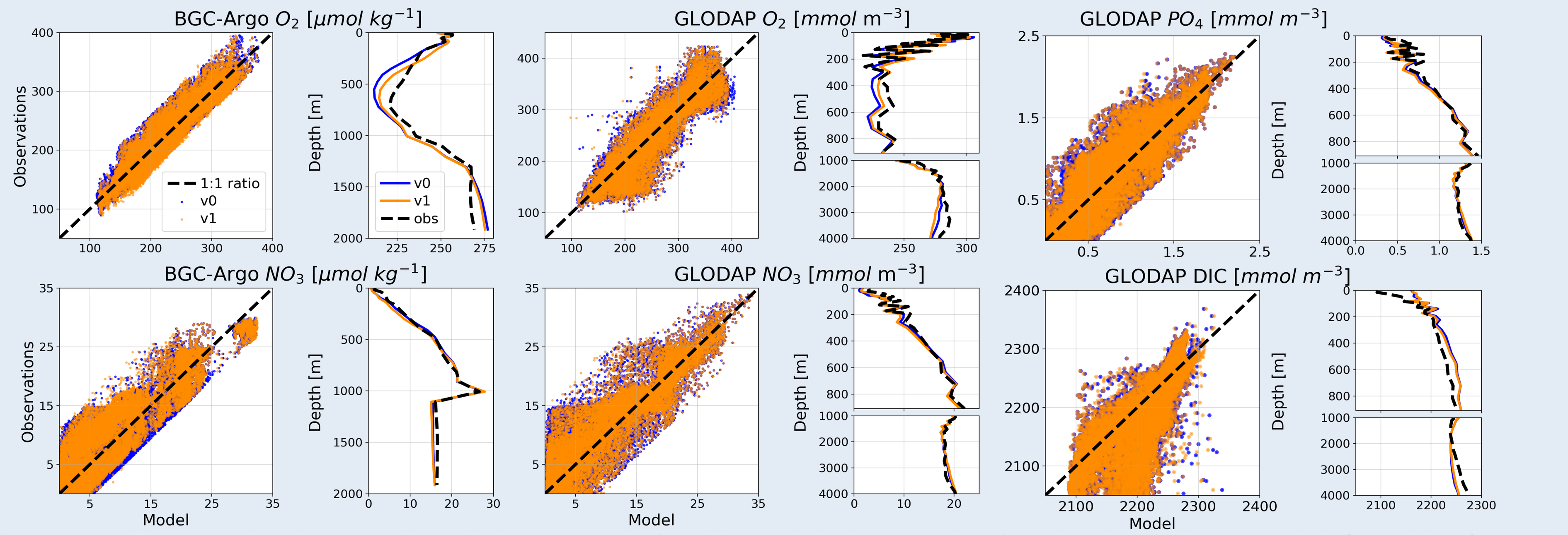

Figure 3. For each observational dataset, [left] all model-data pairs for the baseline model (v0, blue) and optimized model (v1, orange) plotted on a 1:1 axis and [right] the 3-D-averaged vertical profile of all baseline model (blue line), optimized model (orange line), and observations (dashed black line) data.